Journal of Advanced Research in Applied Sciences and Engineering Technology

Journal homepage:
https://semarakilmu.com.my/journals/index.php/applied_sciences_eng_tech/index
ISSN: 2462-1943

Zero-Biasing Split Ring Resonator using Metamaterial Element for High Gain Superstrates Ultra-Wideband Antenna

Nur Amirah Othman[1], Mohd Aminudin Jamlos[1,*], Wan Azani Wan Mustafa[2], Mohd Faizal Jamlos[3], Mohamad Nur Khairul Hafizi Rohani[2], Syahrul Affandi Saidi[2], Hidayath Mirza[4]

[1] Faculty of Electronic Engineering Technology, Universiti Malaysia Perlis, Perlis, Malaysia
[2] Faculty of Electrical Engineering Technology, Universiti Malaysia Perlis, Perlis, Malaysia
[3] Department of Electrical, College of Engineering, Universiti Malaysia Pahang, Malaysia
[4] Department of Electrical Engineering, Jazan University, Saudi Arabia

ARTICLE INFO

Article history:
Received 24 December 2022
Received in revised form 1 March 2023
Accepted 7 March 2023
Available online 24 March 2023

Keywords:
Zero biasing; metamaterial antenna; high gain; ultra-wideband antenna

ABSTRACT

Complex materials with artificial structures known as metamaterials (MTM) have unique properties that draw several scientists to use them in a variety of research fields. In addition, MTM can go beyond some of the restrictions placed on tools used in technical practise while improving the characteristics of microwaves. The Internet of Things (IoT) application calls for the construction of zero-index Split Ring Resonator (SRR) MTM element superstrates with an ultra-wideband antenna. Keep in mind that the MTM simulates behaviour that is not found in nature, namely the zero-reflection phase (dB) on the resonance frequency. For this project, an antenna with an SRR MTM unit cell operating at 2.70 GHz is built. The SRR has four inductance-related loops (r1, r2, r3, and r4), and gaps (slots) are added to the ring to produce the capacitance effect. Parametric research has been done for the SSR in the interim to identify the best design with zero indexes, permittivity and permeability at the desired frequency. The MTM unit cells array design's 7 x 4 and 10 x 5 dimensions achieved a dB of 0° at the 2.70 GHz frequency range. A 7 x 4 MTM unit cell makes up the first design, MTM Antenna Design 1, which at 2.70 GHz recorded a gain of 5.70 dB and a return loss (S11) of -20.007 dB. The return loss (S11) at a frequency of 2.70 GHz was -19.734 dB in the second design, an MTM antenna consisting of 10 x 5 MTM unit cells, which recorded a gain of 5.66 dB.

1. Introduction

Artificial electromagnetic metamaterials (MTM) have piqued interest in recent years. Electric permittivity and magnetic permeability can be used to describe electromagnetic MTM according to the effective medium theory. It has been realized the artificially electric plasma uses a metallic wire whose ε is negative [1] while the artificially magnetic plasma whose μ is negative [2]. Apart from that, MTM is a recently developed artificial material [1] that displays negative μ and negative ε. It can be isolated into four kinds of comparative with μ and ε: Double Negative (DNG) medium, Epsilon

* *Corresponding author.*
E-mail address: mohdaminudin@unimap.edu.my

https://doi.org/10.37934/araset.30.1.321330

Negative (ENG) medium, Mu Negative (MNG) medium, and Double Positive (DPS) medium. Keep in mind that DPS media will be played when the texture includes both and is located very close to the edge of nothing. These media are also referred to as Right-Handed Metamaterials (RHM). Greek terminology for possessing qualities that are superior to those of regularly occurring materials is called meta [2-4]. MTM was first developed in 1967 [2] by the Russian theorist Victor Veselago, who was inspired by the fictitious anticipation of a designed material that continuously displays negative and negative. The MTM subsequently gained popularity among scientists at that time. As a result, Pendry stated that MTM is supported by the split ring resonator in 1999 [5], and Smith demonstrated and approved the MTM concept in 2000 [6].

MTM are artificial materials whose qualities can be inferred both from its component parts and from their main use. For hundreds of years, analysts have been incredibly interested in MTM, which is close to a zero-index of refraction [7-9]. Based on the limits of the significant flaw inserted inside the false design, a Zero-Index Metamaterial (ZIM) is typically meant to function as a reflector or a transmitter [7]. Through the use of various cellular structures and substrate materials, MTM opened the door to the realisation of all material attributes [3, 4]. Zero /index is a distinctive material parameter that stands out among the other uncommon material parameters supplied by MTM. It can result in a variety of intriguing occurrences and applications that show how effective ZIM can improve uniform fields [5-7]. Recent research suggests that ZIM's distinctive features may have cleared the way for the development of revolutionary high-gain antennas. In addition, ZIM frequently functions as a reflector or transmitter, depending on the limits of the significant flaw implanted inside the fake structure [12]. An intriguing subclass of MTM known as zero-index media has structures with a sufficient element zero of refraction (at the frequency of interest). Else, they will be incorporated as MTM in principle. It has been suggested that ZIM are frequently employed to limit the far-field example of an antenna inserted inside the medium, to change over bent wavefronts into plane ones, and to style postpone lines. As of late, epsilon-close-to-zero (ENZ) materials have likewise been wanted to work on the productivity of certain waveguides and to downsize the reflection coefficient at a crossing point or curve [13].

Based on Snell's law, it is considered an incident ray on an interface of the ZIM with grazing incidence that comes from a source inside ZIM. A near-zero-index ray in the media will be refracted in a direction that is very close to normal. Note that the lower the optical index is, the closer the normal direction is. Enoch *et al.,* are the first to realize high directive radiation by employing a monopole source embedded in ZIM, thus confining the radiated energy to a small solid angle [10]. After the work of Enoch, [11] proposed a lefthanded MTM as a substrate for designing directional radiation. Through the control of the structure's geometry, the zero-index frequency can be tuned to the desired specification to produce directional emission. In addition, other works about directive radiations employing ZIM were also studied. However, in the previous references, the directive antennas based on ZIM operate at a single frequency or a narrowband frequency [12]. Note that a ZIM is not coordinated to free space except if the ε and permeability are always zero, leading to the reflectance being frequently high. A major exemption for the current guideline may emerge when an actual element of the texture is electrically little. Nonetheless, this restriction could likewise be too serious and doubtlessly applicable, so investigate the probability of planning indexless media adjusted to free space. A non-attractive material with a ε near the very edge of zero is rapidly accessible [13].

Various well-known techniques are used to produce MTM structures, such as the Split Ring Resonator (SRR) [8-10], which is a structure made by planning microstructures known as "atoms" or "cells." It will be possible to create these "atoms" or unit cells using electrical, nonelectrical, or dielectric materials. In addition, a unit MTM cell must have a dimension of a compelling

homogeneous structure that is abundant and smaller than the directed wavelength. A smaller loop inside a much larger loop frames the SRR, and slots are added to each loop at its opposing ends [8]. Further gaps (splits) from the ring introduce capacitance, allowing for the manipulation of the structure's resonant property. It is regarded as a perfect magnetic conductor throughout a restricted variety of frequencies. Furthermore, in place of the magnetic conductors provide a reflection phase (dB) of incident electric powered fields, thus may permit it to adorn the performance of antennas. MTM should behave as a homogeneous plane for the antenna on the antenna's operating frequency. This allows the in-phase reflected image reaction and avoids unwanted interactions with single resonator cells at intervals of the MTM structure [11]. Various kinds of SRR are frequently considered to style as an MTM to work at various frequencies. For example, Outlined Square rings, different C examples, square and circular designs, and so forth are believed to be MTM.

2. Zero-Index Split Ring Resonator Metamaterial (MTM) Element Design

The suggested antenna design architecture begins with a Metamaterials (MTM) unit cell, resulting in a unit cell design with a resonance characteristic in the frequency range of 3.1 GHz to 10.6 GHz. For designing MTM structures, a number of well-known techniques are employed, including Split Ring Resonator (SRR) [15–17]. The first unit cell in this study is based on an SRR structure. There are four loops in the SRR: Slots are inserted onto each loop at the opposing ends to create a smaller loop inside a larger one [16, 18]. According to [15–19], and as shown in Figure 1, a parallel LC (inductor and capacitor) circuit is modelled for an MTM unit cell SRR.

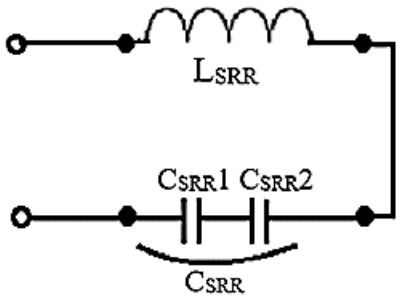

Fig. 1. Lumped element equivalent circuit SRR Unit Cell

The Nicholson-Ross-Weir (NRW) Techniques permit a direct estimation of permittivity (ε) and permeability (μ) from the s-parameter. It is the method that undergoes such a metamorphosis the most frequently. The NRW recovery material boundary extraction method was used to verify the MTM trademark. A number of strategies also rely on estimates (mathematical simulation) of a planar material example's reflection and transmission coefficients [20-22].

Where z, the wave impedance; ε, the relative effective permittivity; μ, the permeability; n, the refractive index; k0, the wavenumber of the incident wave in the free space; d, the slab thickness of the MTM.

Negative can be created by reacting a magnetically resonant structure like an SRR with a perpendicular magnetic field. Capacitance can also be controlled by adding gaps (splits) to the ring, which allows for the structure's resonant characteristic to be controlled. Figure 2 depicts the modification of the first unit cell, which is rectangular and SRR. 2. Keep in mind that the change is the outer ring's loop being closed, which lowers the SRR's series capacitance. Additionally, a wider

backwards-wave passband is made possible by increasing the coupling between the outer and inner rings when the outer ring is closed [16].

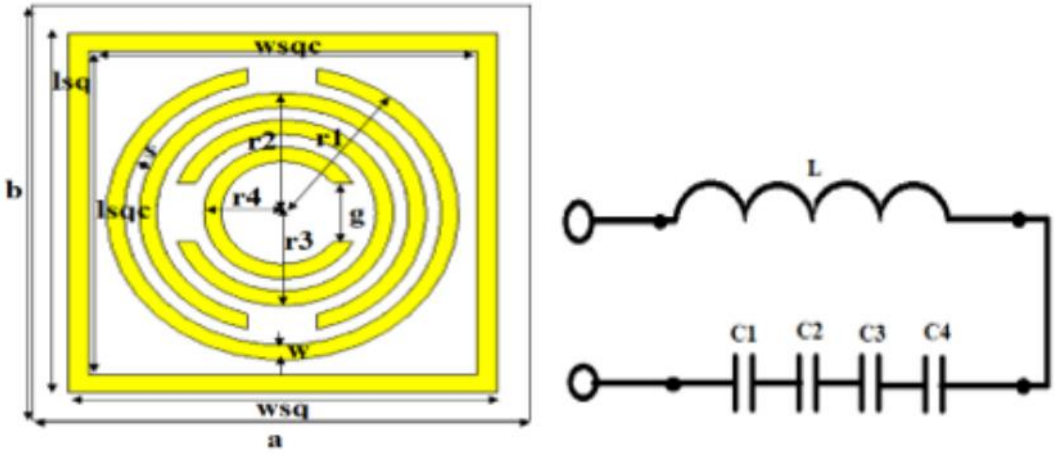

(a) (b)

Fig. 2. (a) The geometry of the proposed front view of MTM Unit Cell (b) Equivalent Circuit Diagram of MTM Unit Cell

The design that was used for the test was placed in between two waveguide terminals that were at the top and bottom of the z-axis, respectively. In addition, a z-axis electromagnetic wave was energized. The dividers were subjected to an exquisitely leading attractive limit condition with the dividers facing the y-axis, and an exquisitely directing electrical limit condition was applied with the dividers facing the x-axis [23]. A set was used to validate every setting for the x, y, and z axes, particularly the Unit Cell Boundary in Figure 3.

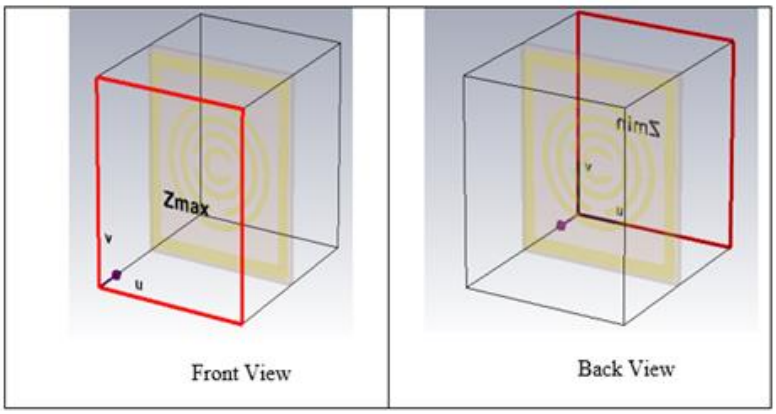

Fig. 3. The perspective source waveguide port for unit cell MTM

Table 1 and Figure 4 demonstrate the optimized dimension of the SRR unit cell simulated using Computer Simulation Technology (CST) software.

Table 1
Dimension for SRR Unit Cell

Parameter	Dimension	Parameter	Dimension
a	15.7	w	0.5
b	15.7	r1	4.525
wsq	7.294	r2	3.6
lsq	7.294	r3	2.675
wsqc	6.0	r4	7.76
lsqc	6.0	c	2.0

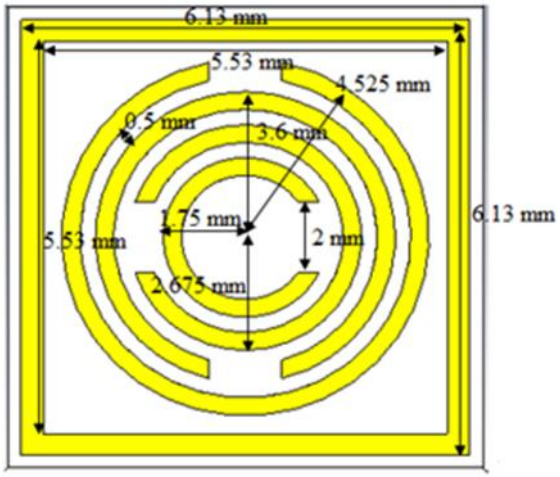

Fig. 4. Dimension for SRR Unit Cell

As a result, the SRR unit cell is assembled into 110 x 65 mm2 array structures. The 7 x 4 unit cell and the 10 x 5 unit cell are the two components of the MTM plane plan, as depicted in Figure 5. In the meantime, the optimal dimensions for MTM unit cell components are displayed in Table 2.

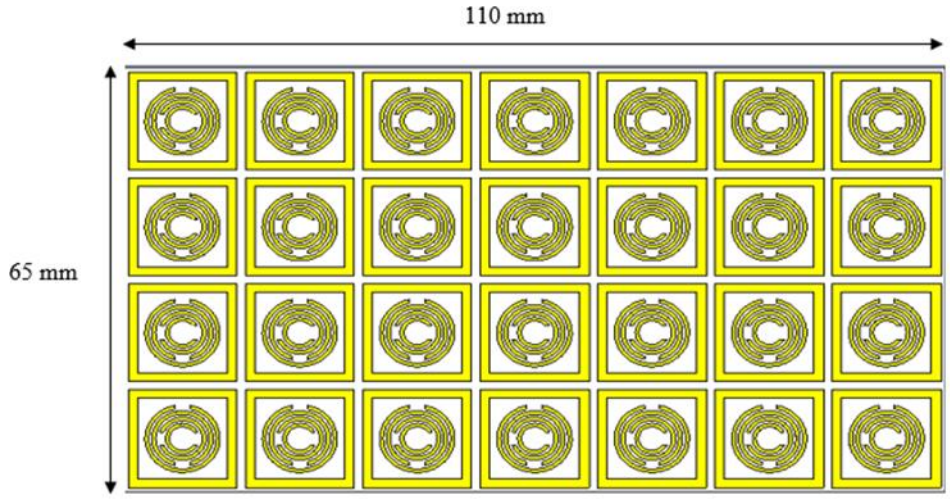

(a)

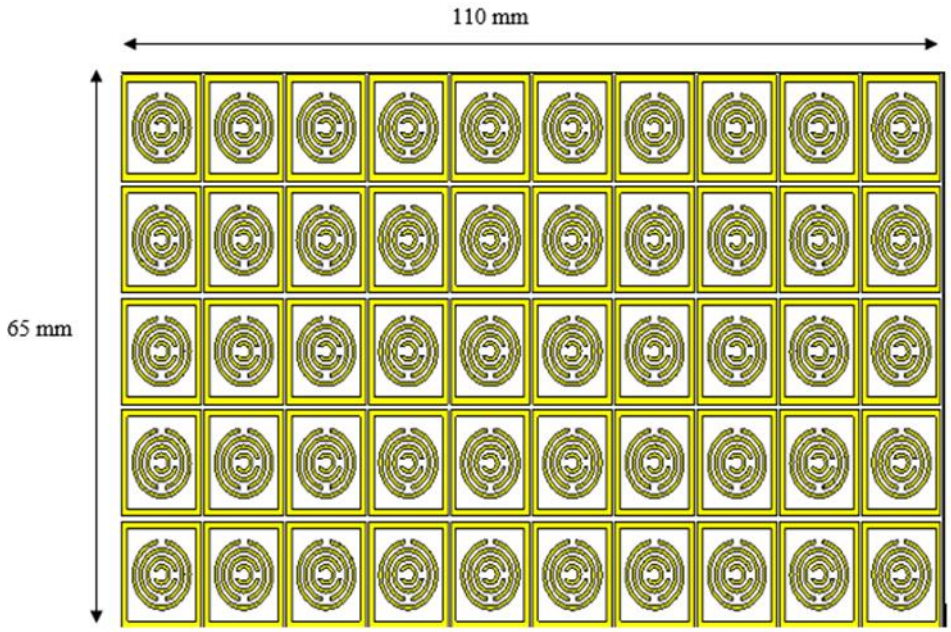

(b)

Fig. 5. (a) Simulated MTM 7 x 4 unit cell Plane, (b) Simulated MTM 10 x 5 unit cell Plane

Table 2
Dimension for SRR Unit Cell

7 x 4 mm2 (28-unit cell)	Parameter	Dimension	Parameter	Dimension
	a	15.7	w	0.5
	b	15.7	r1	4.525
	wsq	7.294	r2	3.6
	lsq	7.294	r3	2.675
	wsqc	6.0	r4	7.76
	lsqc	6.0	c	2.0
10 x 5 mm2 (50-unit cell)	Parameter	Dimension	Parameter	Dimension
	a	11.0	w	0.4
	b	12.6	r1	3.525
	wsq	5.31	r2	2.6
	lsq	6.01	r3	1.675
	wsqc	4.6	r4	0.75
	lsqc	5.2	C	1.0

3. Zero-Index Split Ring Resonator Metamaterial (MTM) Element Performances

CST software was used to simulate the MTM unit cell in light of the FDFD approach to determining the S-parameter [24]. The design that was used for the test was between two waveguide terminals that were at the top. An electromagnetic wave was directed along the z-axis down to the lower part of the design. The partitions located in opposition to the x-axis were subjected to an extremely directing electrical limit condition. A frequency-domain solver was used to imitate this MTM structure, and an impeccably leading attractive limit condition was applied to the walls opposite the y-axis. utilizing the simulation CST software to extract the effective constitutive parameters from S21 and S11, such as the refractive index (nr), the relative effective permittivity (r), and the relative effective permeability (r) [6].

The details of the simulated minimum transmission frequency with various turns in the SRR have been extracted from the simulation in order to determine the proposed SRR based on the length of the outer ring, inductance, and capacitance. It is important to note that Roger's (RT 5880) substrate was used to carry the design. When the number of SRR rings (N) is 2, 3, 4, or 5, and the square shape is added, the minimum frequency of the transmission of resonant particles is observed. In addition, the resonant frequency is observed, as depicted in Figure 6. In a similar manner, the values of the inductance and capacitance in the SRR that looks at the minimum transmission frequency are calculated. The comparison between the SRR simulation frequency and the calculated minimum transmission frequency is shown in Table 3.

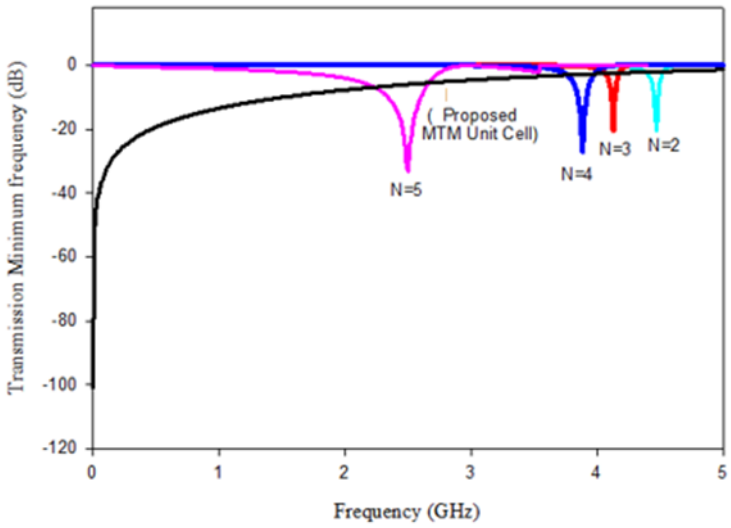

Fig. 6. The minimum transmission frequency with different turns in SRR

Table 3
Calculated and Simulated Transmission Minimum Frequency SRR

No of rings (N)	Length of Outer Ring (l) (mm)	L (nH)	C (pF)	Transmission Minimum frequency (GHz) (Calculated)	Transmission Minimum frequency (GHz) (Simulated)
2	1.675	2.03543	0.306299	6.37	4.56
3	2.60	2.94498	0.48377	4.22	4.02
4	3.525	3.85453	0.671297	3.13	3.88
5	4.0	5.05161	0.827856	2.46	2.50
The Proposed MTM Unit Cell	5.31	2.66979	0.932183	-	2.70

To achieve an operating frequency of 2.70 GHz, the performance of the proposed MTM cell design depends on the width and length of the SR. The proposed MTM Antenna Design has been identified for Parametric Study 5, with an operating frequency of 2.70 GHz and a dB angle of 0°. The frequency for Parametric Study 1 is 2.50 GHz absent the width and length of SR. Aside from that, the dB of 0° at 2.70 GHz has been achieved by altering the width and length of the SR parameters for each of these Parametric Studies (2–5).

The dB results demonstrate that the MTM unit cell is a reflective material close to 2.70 GHz. Additionally, the spatiality of the correlation (anisotropy or asymmetry) can be seen in the phase

behavior of the S-parameter. Resonant frequency is defined as the frequency at which phase S11 crosses the 0° axis (f0 = f | phase(S11) = 0°). Because they are the only parameters of a substance that appear within the dispersion equation, permittivity and magnetic are the fundamental feature quantities that govern the advancement of electromagnetic waves in the matter. Aside from that, both scientific and industrial applications necessitate the measurement of these advanced parameters. One of the essential tasks for defining the MTM is to extract these parameters.

Simulation software provides distinctive or unique features as an expressed antecedent. The real, nr, and wave impedances of MTM 7 x 4 unit cells and 10 x 5 unit cells were then calculated using NRW Techniques for the comparative analysis.

At an operating frequency of 2.70 GHz, the simulated and calculated results presented in Table 4 showed that the achieved real, nr, and wave impedances of the 7 x 4 unit cell and the 10 x 5 unit cell were in good agreement. At MTM 7 x 4 unit cells and 10 x 5 unit ells' frequency bands, the real, nr, and wave impedance values were also very close to zero. Although the simulator uses more complex and precise equations to determine the operation, it is likely more accurate than hand calculation, even though the values are slightly different. Nevertheless, the MTM was ZIM, as demonstrated by the values in the first quadrant of MTM types in both the simulated and measured results.

Table 4
The results of the achieved real permittivity, permeability, refractive index, and wave impedance

7 x 4 MTM Unit Cell		Real Values of MTM Unit Cell	10 x 5 MTM Unit Cell	
Simulated	Calculated		Simulated	Calculated
0.00365	0.14330	Permittivity	0.0455	0.12663
0.00541	0.17067	Permeability	0.00678	0.17089
0.00141	0.1564	Refractive Index	0.0176	0.14710
0.385	0.1489	Wave Impedance	0.386	0.14816

The ZIM, also known as Double Positive (DPS) media, can be planned by dispersing the metallic or dielectric particles by embedding the metallic or dielectric bar (network) in the subwavelength metallic or dielectric structure. The ZIM, also known as the principal quadrant of MTM characteristic, can be obtained from every electric MTM close to zero and every attractive MTM with almost zero.

5. Conclusions

The Zero-Index Metamaterial (ZIM) element's Split Ring Resonator (SRR) design is successful. The SRR's optimal width and length have been determined through a parametric study to achieve zero indexes at the desired frequency of 2.7 GHz. Aside from that, the SRR has four distinct loops and optimized dimensions of 7.29 mm and 6.0 mm for width and length, respectively. At the desired frequency of 2.7 GHz for low-frequency applications, specifically GHz ranges, the SRR successfully recorded zero indexes (phase). The 7 x 4 unit cell and the 10 x 5 unit cell are the two array structures for the SRR unit cell. At the desired frequency of 2.70 GHz, note that both array configurations recorded zero indexes (phase) and positive on the point of close to zero results for permittivity and permeability. When comparing the two antennae made of Metamaterials (MTM) element superstrates, one can see that the shape of the 7 x 4 MTM element has a low number of unit cells and a high gain, making it a better choice than the 10 x 5 MTM element.

Acknowledgement
This work was supported by the Ministry of Higher Education Malaysia under the Fundamental Research Grant Scheme (FRGS/1/2018/ICT06/UNIMAP/02/1).

Funding Statement
This work was funded by the Ministry of Higher Education Malaysia under the Fundamental Research Grant Scheme (FRGS/1/2018/ICT06/UNIMAP/02/1).

Conflicts of Interest
The authors declare that they have no conflicts of interest to report regarding the present study.

References
[1] Liu, Yahong, Xiaojing Guo, Shuai Gu, and Xiaopeng Zhao. "Zero index metamaterial for designing high-gain patch antenna." *International Journal of Antennas and Propagation* 2013 (2013). https://doi.org/10.1155/2013/215681
[2] Zhou, Jiangfeng, Lei Zhang, Gary Tuttle, Thomas Koschny, and Costas M. Soukoulis. "Negative index materials using simple short wire pairs." *Physical Review B* 73, no. 4 (2006): 041101. https://doi.org/10.1103/PhysRevB.73.041101
[3] Hou, Quanwen, Hangfei Tang, Yahong Liu, and Xiaopeng Zhao. "Dual-frequency and broadband circular patch antennas with a monopole-type pattern based on epsilon-negative transmission line." *IEEE Antennas and Wireless Propagation Letters* 11 (2012): 442-445. https://doi.org/10.1109/LAWP.2012.2195470
[4] Smith, D. R., D. C. Vier, Th Koschny, and C. M. Soukoulis. "Electromagnetic parameter retrieval from inhomogeneous metamaterials." *Physical review E* 71, no. 3 (2005): 036617. https://doi.org/10.1103/PhysRevE.71.036617
[5] Yao, Yuan, Xing Wang, and Junsheng Yu. "Multiband planar monopole antenna for LTE MIMO systems." *International Journal of Antennas and Propagation* 2012 (2012). https://doi.org/10.1155/2012/890705
[6] Zhao, YuChen, GuoBin Wan, HuiLing Zhao, and WenQuan Zheng. "Effects of superstrate with improved SSRRs on the radiation of microstrip antenna." In *2009 3rd IEEE International Symposium on Microwave, Antenna, Propagation and EMC Technologies for Wireless Communications*, pp. 51-54. IEEE, 2009. https://doi.org/10.1109/MAPE.2009.5355556
[7] Zhou, Hang, Zhibin Pei, Shaobo Qu, Song Zhang, Jiafu Wang, Zhangshan Duan, Hua Ma, and Zhuo Xu. "A novel high-directivity microstrip patch antenna based on zero-index metamaterial." *IEEE Antennas and wireless propagation letters* 8 (2009): 538-541. https://doi.org/10.1109/LAWP.2009.2018710
[8] Hagness, Susan C., Allen Taflove, and Jack E. Bridges. "Two-dimensional FDTD analysis of a pulsed microwave confocal system for breast cancer detection: Fixed-focus and antenna-array sensors (vol 45, pg 1470, 1998)." (1999). https://doi.org/10.1109/TBME.1999.748990
[9] Hossain, Toufiq Md. "Symmetric Wideband Five Port Reflectometer for Microwave-imaging Based Brain Injury Diagnosis." PhD diss., School of Computer and Communication Engineering, 2018.
[10] Abbosh, A. M., A. Zamani, and A. T. Mobashsher. "Real-time frequency-based multistatic microwave imaging for medical applications." In *2015 IEEE MTT-S 2015 International Microwave Workshop Series on RF and Wireless Technologies for Biomedical and Healthcare Applications (IMWS-BIO)*, pp. 127-128. IEEE, 2015. https://doi.org/10.1109/IMWS-BIO.2015.7303811
[11] Abdul-Sattar, Zubaida. "Experimental analysis on effectiveness of confocal algorithm for radar based breast cancer detection." PhD diss., Durham University, 2012.
[12] Fear, Elise C., J. Bourqui, C. Curtis, D. Mew, B. Docktor, and C. Romano. "Microwave breast imaging with a monostatic radar-based system: A study of application to patients." *IEEE transactions on microwave theory and techniques* 61, no. 5 (2013): 2119-2128. https://doi.org/10.1109/TMTT.2013.2255884
[13] Fear, Elise C., Susan C. Hagness, Paul M. Meaney, Michal Okoniewski, and Maria A. Stuchly. "Enhancing breast tumor detection with near-field imaging." *IEEE Microwave magazine* 3, no. 1 (2002): 48-56.
[14] Khor, Wee Chang, Aslina Abu Bakar, and Marek E. Bialkowski. "Investigations into breast cancer detection using ultra wide band microwave radar technique." In *2009 Asia Pacific Microwave Conference*, pp. 712-715. IEEE, 2009. https://doi.org/10.1109/APMC.2009.5384238
[15] Mendhe, Shridhar E., and Yogeshwar Prasad Kosta. "Metamaterial properties and applications." *International Journal of Information Technology and Knowledge Management* 4, no. 1 (2011): 85-89.
[16] Islam, Md Moinul, Mohammad Tariqul Islam, Mohammad Rashed Iqbal Faruque, Md Samsuzzaman, Norbahiah Misran, and Haslina Arshad. "Microwave imaging sensor using compact metamaterial UWB antenna with a high correlation factor." *Materials* 8, no. 8 (2015): 4631-4651. https://doi.org/10.3390/ma8084631

[17] Islam, Md Moinul, Mohammad Tariqul Islam, Md Samsuzzaman, Mohammad Rashed Iqbal Faruque, Norbahiah Misran, and Mohd Fais Mansor. "A miniaturized antenna with negative index metamaterial based on modified SRR and CLS unit cell for UWB microwave imaging applications." *Materials* 8, no. 2 (2015): 392-407.

[18] Islam, Md Moinul, Mohammad Tariqul Islam, Md Samsuzzaman, Mohammad Rashed Iqbal Faruque, Norbahiah Misran, and Mohd Fais Mansor. "A miniaturized antenna with negative index metamaterial based on modified SRR and CLS unit cell for UWB microwave imaging applications." *Materials* 8, no. 2 (2015): 392-407. https://doi.org/10.3390/ma8020392

[19] Jais, M. I., M. F. Jamlos, M. Jusoh, T. Sabapathy, M. K. A. Nayan, A. Shahadah, Hazliza A. Rahim, I. Ismail, and F. A. A. Fuad. "1.575 GHz dual-polarization textile antenna (DPTA) for GPS application." In *2013 IEEE Symposium on Wireless Technology & Applications (ISWTA)*, pp. 376-379. IEEE, 2013. https://doi.org/10.1109/ISWTA.2013.6688808

[20] Rochman, Refada Adyansya, Sayekti Wahyuningsih, Ari Handono Ramelan, and Qonita Awliya Hanif. "Preparation of nitrogen and sulphur Co-doped reduced graphene oxide (rGO-NS) using N and S heteroatom of thiourea." In *IOP Conference Series: Materials Science and Engineering*, vol. 509, no. 1, p. 012119. IOP Publishing, 2019. https://doi.org/10.1088/1757-899X/557/1/012002

[21] Shao, Wenyi, and Ryan S. Adams. "UWB microwave imaging for early breast cancer detection: A novel confocal imaging algorithm." In *2011 IEEE International Symposium on Antennas and Propagation (APSURSI)*, pp. 707-709. IEEE, 2011.

[22] Li, Xu, and Susan C. Hagness. "A confocal microwave imaging algorithm for breast cancer detection." *IEEE Microwave and wireless components letters* 11, no. 3 (2001): 130-132. https://doi.org/10.1109/7260.915627

[23] XIAO, Xia, and Takamaro KIKKAWA. "UWB Imaging for Early Breast Cancer Detection by Confocal Algorithm." In *Extended abstracts of the... Conference on Solid State Devices and Materials*, (2007): 976-977.

[24] Jamlos, Mohd Aminudin, Nurasma Husna Mohd Sabri, Mohd Faizal Jamlos, Wan Azani Mustafa, Syed Zulkarnain Syed Idrus, Mohamad Nur Khairul Hafizi Rohani, Khairul Najmy Abdul Rani, and Mohd AL Hafiz Mohd Nawi. "5.8 GHz Circularly Polarized Rectangular Microstrip Antenna Arrays simulation for Point-to-Point Application." *Journal of Advanced Research in Applied Sciences and Engineering Technology* 28, no. 3 (2022): 209-220. https://doi.org/10.37934/araset.28.3.209220